Nanophotonics of Hexagonal Lattice GaN Crystals Fabricated using an Electron Beam Nanolithography Process

In Goo Lee[1], Keunjoo Kim[1,#], Sang Cheol Jeon[2], Jin Soo Kim[2] and Hee Mok Lee[2]

1 Department of Mechanical Engineering and Research Center of Industrial Technology, Chonbuk National University, Jeonju 561-756, South Korea
2 Lithography Team, National Nanofab Center, KAIST, Daejon, South Korea
Corresponding Author / E-mail: kimk@chonbuk.ac.kr, TEL: +82-63-270-2317, FAX: +82-63-270-2315

KEYWORDS: Nanophotonics, Nanolithography, Photonic crystal, GaN semiconductor

A thin GaN semiconducting film that grows on sapphires due to metalorganic chemical vapor deposition was machined for nanophotonic applications. The thin film had multilayered superlattice structures, including nanoscaled InGaN layers. Eight alternating InGaN/GaN multilayers provided a blue light emission source. Nanoscaled holes, 150 nm in diameter, were patterned on polymethylmethacrylate (PMMA) film using an electron beam lithography system. The PMMA film blocked the etching species. Air holes, 75 nm in diameter, which acted as blue light diffraction sources, were etched on the top GaN layer by an inductively coupled plasma etcher. Hexagonal lattice photonic crystals were fabricated with 230-, 460-, 690-, and 920-nm pitches. The 450-nm wavelength blue light provided the nanodiffraction destructive and constructive interferences phenomena, which were dependent on the pitch of the holes.

Manuscript received: October 10, 2005 / Accepted: January 21, 2006

NOMENCLATURE

$\mathbf{E}(\mathbf{r})$ = electric field
$\mathbf{H}(\mathbf{r})$ = magnetic field
$\mathbf{k}_{//}$ = wave vectors in a plane
k_z = wave vector in the z-direction
n = photonic band number
$\mathbf{U}(z)$ = z-periodic function
λ = wavelength
ω = frequency

1. Introduction

Recent advances in nanofabrication technologies have resulted in useful applications for nanodevices. One such application is nanophotonics, in which nanoscaled periodic structures are used to obtain the appropriate characteristics of photonic crystals. Photonic crystals with a lattice constant comparable to the wavelength of light can influence the spontaneous emission of light due to the formation of a photonic band gap.[1,2] In semiconductor materials, a high optical refractive index prevents light extraction, providing a small external quantum efficiency in optoelectronic devices.[3,4] Thus, these crystals have potential applications in optoelectronic devices such as light emitting diodes (LEDs) and laser diodes (LDs).

III-Nitride wideband gap materials have been extensively investigated for optoelectronic applications for the ultraviolet to visible light spectrum. The light extraction efficiency of an InGaN/GaN multiple quantum well structure LED can be enhanced by introducing photonic crystals.[5-7] However, the dependence of the photonic crystal lattice constant on the wavelength of the light is still uncertain in the context of the external quantum efficiency.

In this paper, we examine the optically pumped light emission properties in a LED structure. These are correlated with the lattice size of the photonic crystals. The photoluminescence intensity was measured for various photonic crystal lattice constants. The crystals were fabricated by etching a thin GaN film into hexagonal or triangular holes.

2. Photonic Crystals

2.1 Basic Theory

A two-dimensional photonic crystal is periodic along two axes. A typical specimen consisting of a triangle lattice of dielectric holes is shown in Fig. 1. For certain values of the hole spacing, this crystal can have a photonic band gap in the xy-plane. No extended states are permitted inside this gap, and incident light from any direction in the plane is reflected.

A two-dimensional photonic crystal has a discrete translational symmetry in the xy-plane and is homogeneous in the z-direction, with plane wave characteristics for the wave vector k_z. By applying Bloch's theorem for the wave vector $\mathbf{k}_{//}$ in the xy plane of the Brillouin zone and using band number n for the frequency mode, the electromagnetic field can be written as follows.[2]

$$\mathbf{H}_{(n,kz,\mathbf{k}//)}(\mathbf{r}) = \exp(i\,\mathbf{k}_{//}\cdot\ \rho)\exp(i\,k_z z)\,\mathbf{U}_{(n,kz,\mathbf{k}//)}(\rho)$$

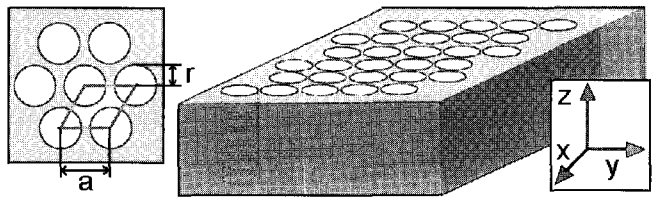

Fig. 1 Two-dimensional photonic crystal with air holes in a thin GaN film. The holes have radius r and dielectric constant $\varepsilon = 1$. The left inset shows the triangular lattice unit cell with a lattice constant a[2]

Here, $\mathbf{U}(\rho)$ is the periodic function $\mathbf{U}(\rho) = \mathbf{U}(\rho + \mathbf{R})$ for all lattice vectors $\mathbf{R}$. If $k_z = 0$ so that light propagates strictly in the xy-plane, then the system is invariant under reflections through the xy-plane. This mirror symmetry allows us to classify the modes by separating them into two distinct polarizations. Transverse electric (TE) modes have $\mathbf{H}$ normal to the plane $\mathbf{H} = \mathbf{H}(\rho)\underline{\mathbf{z}}$, and $\mathbf{E}$ in the plane $\mathbf{E}(\rho) \cdot \underline{\mathbf{z}} = 0$. Transverse magnetic (TM) modes have just the reverse: $\mathbf{E} = \mathbf{E}(\rho)\underline{\mathbf{z}}$ and $\mathbf{H}(\rho) \cdot \underline{\mathbf{z}} = 0$.

The arrangement of the holes is very important when forming complete band gap overlapping for both polarizations. A TM band gap is favored in a lattice of isolated high-dielectric regions, such as nanorods, while a TE band gap is favored in a connected lattice, such as holes. At first glance, it appears impossible to arrange a photonic crystal with both isolated spots and connected regions of dielectric material. However, a triangular lattice of air holes provides spots between holes with large enough radii. These localized high dielectric spots are connected to adjacent spots by narrow veins. The band structure for this lattice, shown in Fig. 2, has a photonic band gap for both the TE and TM polarizations at a normalized frequency of 0.5, indicating that the lattice constant is a half wavelength, $a = \lambda/2$, for a ratio of hole diameters to lattice constant $2r/a = 0.9$.

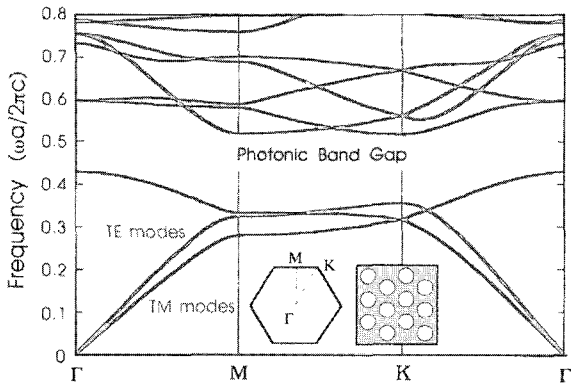

Fig. 2 Complete photonic band structure for the TE and TM modes of a triangular array of air holes ($\varepsilon = 13$). The inset shows the high-symmetry points at the corners of the irreducible Brillouin zone[2]

2.2 Experimental Results

The LED structures were grown using metalorganic chemical vapor deposition on sapphire substrates. After nucleation, a 30-nm-thick buffer layer was grown at a temperature of 520°C. Then a 3-μm-thick n-type GaN layer was deposited on the surface at a temperature of 1130°C. This was followed by a multiple quantum well (MQW) active region consisting of 2-nm-thick InGaN wells and 8-nm-thick GaN barriers emitting at a blue wavelength of 450 nm. The MQW region consisted of eight alternating layers of InGaN wells and GaN barriers, each grown at the same temperature of 790°C. Finally, a 200-nm-thick p-type GaN layer was grown and post-annealed at 700°C for 15 min.

Fig. 3 shows a schematic diagram of the InGaN/GaN photonic crystal LED epitaxial structure. Five different photonic crystal (PX) lattices were manufactured on wafers and subsequently investigated. Since the peak light emission of the LED structure occurs at a blue wavelength of 460 nm, we designed the lattice constants in terms of half and multiple integers of this wavelength: 230, 460, 690, 920, and 1380 nm. The hexagonal PX lattice was formed only on the top p-GaN layer using electron beam nanolithography and inductively coupled plasma (ICP) dry etching. Each PX was patterned for a 500 × 500 μm area. Crystal lattice patterns consisting of circular 150-nm diameter holes with different periodicities were defined on the polymethylmethacrylate (PMMA) initially spun onto the nitride samples. A triangular lattice of holes on a dielectric background has been shown to be one of the most prominent two-dimensional structures that create photonic band gaps.[2] The patterned samples were then developed in a solution of methylisobuthyl ketone and isopropyl alcohol. Subsequent dry etching for nano-machining process was performed for 5 s using an ICP dry etcher.[8-11]

The room-temperature photoluminescence of various PX samples was measured with an incident 40 mW He–Cd laser source activated at a 325-nm wavelength. Images of the PX patterns were investigated using a CD–SEM and an AFM.

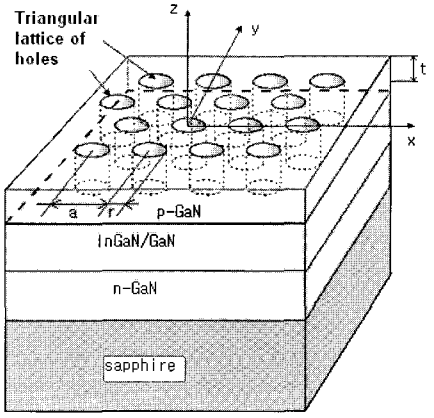

Fig. 3 Schematic diagram of an InGaN/GaN multiple quantum well blue LED photonic crystal structure manufactured on a p-GaN layer

Fig. 4 shows a CD–SEM image of a sample of the PMMA patterns obtained using the electron beam nanolithography. The diameter and pitch of the holes were 150 and 230 nm, respectively. The electron beam removed the PMMA located inside the holes up to a diameter of 143 nm. The CD–SEM image shows also the contrast of the reflected intensity.

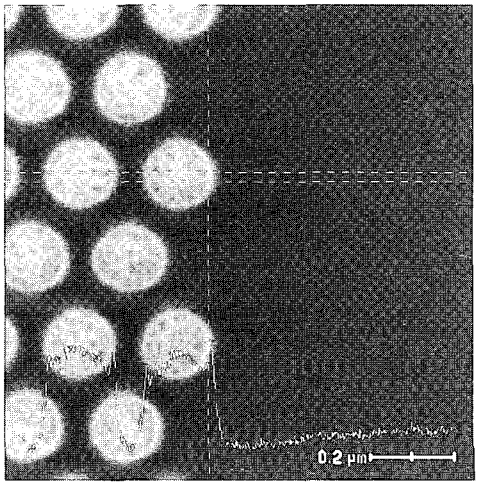

Fig. 4 Patterned nanophotonic crystal structure obtained using electron beam lithography on the PMMA

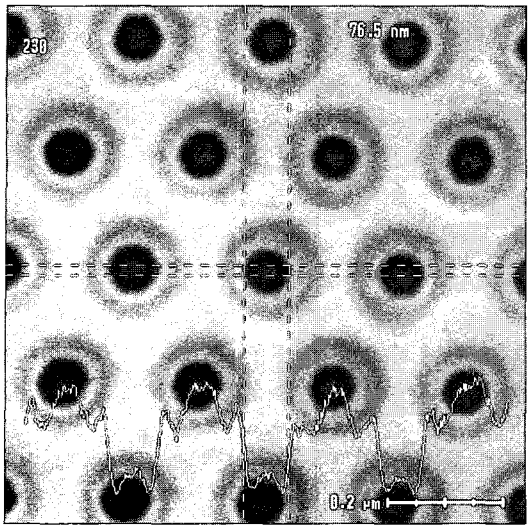

(a) With PMMA

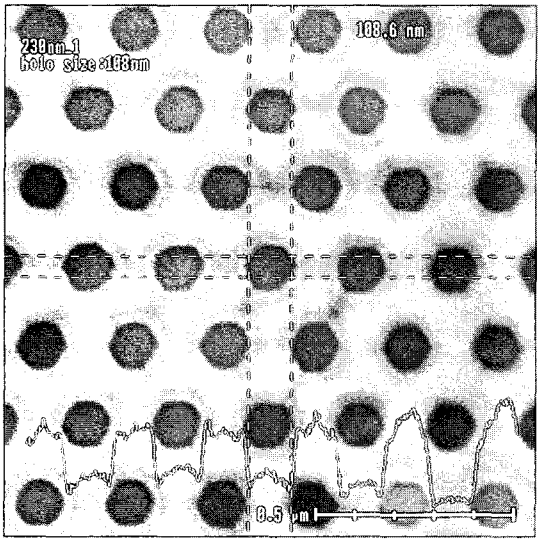

(b) Without PMMA

Fig. 5 Nanophotonic crystal structure after ICP etching

Fig. 5(a) shows a CD–SEM image of a sample that was coated with a PMMA photoresist after the ICP etching process. The pitch of the sample was 230 nm, and the main ICP etching gases were BCl_3 and Cl_2. The 200-nm-thick photoresist blocked the plasma gas so that the resulting craterlike pattern consisted of 150-nm diameter holes that contained smaller 75-nm concentric holes on their lower surfaces. Figure 5(b) shows an image for a similar sample without the PMMA. The GaN photonic crystals formed a very rough surface during the ICP etching process. The holes without PMMA had a 108-nm diameter. The surface roughness and the depth of the holes can be characterized using AFM measurements, which can also be used to visualize the morphological formation of the spots and veins in the hexagonal array of holes.

Fig. 6 shows an AFM image of a sample with a 230-nm pitch. The image shows only spots without holes and holes surrounded by six spots. The diameter of the artificial circles was 152 nm, and the depth of the holes was 34 nm. The slope of the sides of the holes was 18°, and the diameter at the top and bottom of the holes was 314 and 112 nm, respectively.

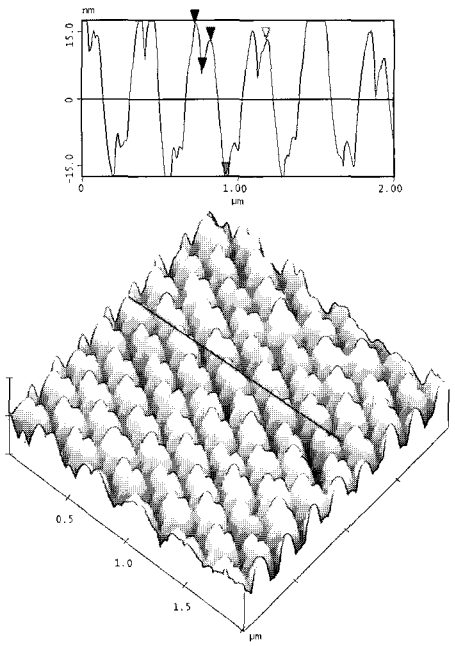

Fig. 6 AFM image of a sample with a 230-nm pitch

The ratio of the lattice constant to the wavelength of the blue light emissions from the quantum well active layer was 0.51. The hole occupation ratio of the radius to the lattice constant ratio was 0.33. For a GaAs photonic crystal, a photonic band gap exists at a lattice constant to wavelength ratio of 0.5 and a radius to lattice constant ratio of 0.45. Therefore, for similar dielectric constants between GaAs (11.4) and GaN (8.9), the sample with a 230-nm lattice constant produced a photonic band gap for both the TE and TM modes, indicating destructive interference.[12,13]

Fig. 7 shows an AFM image of a sample with a 460-nm pitch. The image shows the hexagonal symmetry of the holes surrounded by three peaks. The average diameter and the depth of the holes were 150 and 28 nm, respectively. The deviation of the average hole diameter was 5 nm. The holes were etched with a slope of 9° so that the diameters at the top and bottom of the tapered holes were 210 and 75 nm, respectively. The average roughness of the surface of the photonic crystals was 9.5 nm. The image indicates that the plasma etching species removed the periodic pattern from the entire surface.

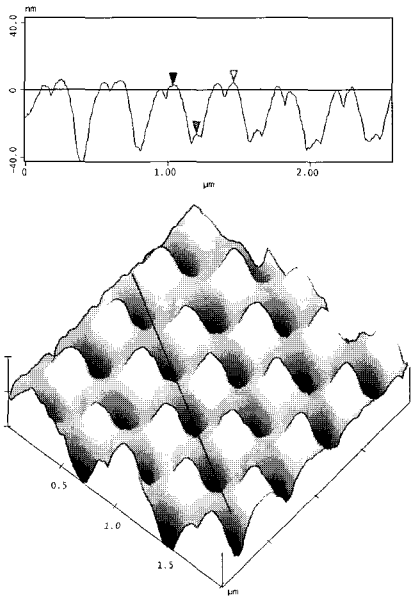

Fig. 7 AFM image of a sample with a 460-nm pitch

The 450-nm blue light photoluminescence from the quantum well active layer passed through the holes. The ratio of the lattice constant to wavelength was 1.02, while the ratio of the hole occupation of the radius to the lattice constant was 0.16. This hole structure provided a TE mode band gap but not a TM mode band gap, formulating constructive interference.

Fig. 8 shows the photoluminescence (PL) spectra for various photonic crystal lattice constants. The blue light peaked at 450 nm and originated from the InGaN/GaN multiple quantum well structure. The PL intensity could be enhanced by introducing photonic crystals with lattice constants greater than the wavelength of the emitted light. But as the lattice constant of a photonic crystal is increased, the PL intensity becomes limited on bare samples without photonic crystals. The PL intensity from the sample with the 460-nm lattice constant was double that of the bare sample. However, the sample with the 230-nm lattice constant provided no PL intensity, indicating the presence of a photonic band gap (PBG) region.[14]

A PBG is formed at a lattice dimension tuned to the half of the lattice constant wavelength (λ /2) as a result of multiple scattering of photons by lattices of periodically varying refractive indices. From a frequency viewpoint, the PBG is characterized by its midgap ratio of $\Delta\omega/\omega_0$ where $\Delta\omega$ is the frequency range encompassing the PBG and ω_0 is the frequency at the middle of the gap (midgap). The midgap frequency for triangular air holes in GaN with a dielectric constant of ε = 8.9 is estimated to occur at a normalized cutoff frequency ($a/\lambda = \omega a/2\pi c$) of 0.5.[2,4] Therefore, light generated in the band gap region with a cutoff frequency of 0.5 can only radiate outward; the lateral propagation modes are prohibited. Modes above the cutoff frequency are coupled to free space, resulting in an enhancement of the light extraction.

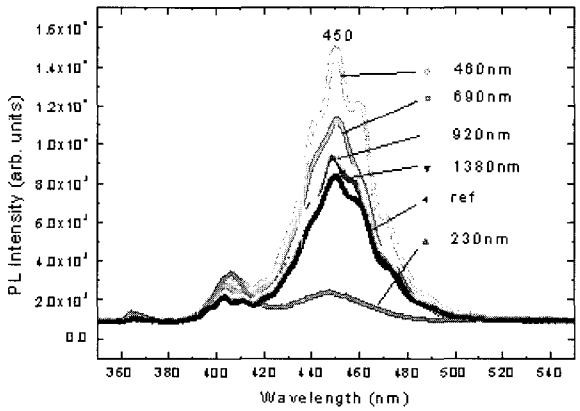

Fig. 8 Photoluminescence spectra for various lattice constants. The bare sample without photonic crystals (ref.) is compared to various samples with photonic crystals

3. Conclusions

Various photonic crystals with normalized frequencies of 0.51, 1.02, 1.53, 2.04, and 3.06 were fabricated on a Mg-doped p-type GaN semiconducting thin film grown on the sapphire using metalorganic chemical vapor deposition. Eight alternating InGaN/GaN multilayers provide the blue light emission source. Nanoscale holes, 150 nm in diameter, were patterned on PMMA film using an electron beam lithography system. Then air holes on the GaN surface, which acted as blue light diffraction sources, were etched in the shape of taped circular columns using an inductively coupled plasma etcher. Blue light with a 450-nm wavelength provided the nanodiffraction phenomenon of destructive interference at a normalized frequency of 0.51, corresponding to a lattice constant of 230 nm.

ACKNOWLEDGEMENT

This work was supported through the Korean Research Foundation Grant (KRF-2004-041-D00296). The nanolithography and ICP etching processes were performed at the National Nanofab Center and Knowledge*on, Inc., respectively.

REFERENCES

1. Purcell, E. M., "Spontaneous Emission Probabilities at Radio Frequencies," Phys. Rev., Vol. 69, p. 681, 1946.
2. Joannopoulos, J. D., Meade, R. D. and Winn, J. N., "Photonic Crystals, Molding the Flow of Light," Princeton University Press, Princeton, 1995.
3. Yablonovitch, E., "Inhibited spontaneous emission in solid-state physics and electronics," Phys. Rev. Lett., Vol. 58, No. 20, pp. 2059-2062, 1987.
4. Lee, Y. J., Kim, S. H., Huh, J., Kim, G. H., Lee, Y. H., Cho, S. H., Kim, Y. C. and Do, Y. R., "A high-extraction-efficiency nanopatterned organic light-emitting diode," Appl. Phys. Lett., Vol. 82, No. 21, pp. 3779-3781, 2003.
5. Oder, T. N., Kim, K. H., Lin, J. Y. and Jiang, H. X., "III-nitride blue and ultraviolet photonic crystal light emitting diodes," Appl. Phys. Lett., Vol. 84, No. 4, pp. 466-464, 2000.
6. Oder, T. N., Shakya, J., Lin, J. Y. and Jiang, H. X., "III-nitride photonic crystals," Appl. Phys. Lett., Vol. 83, No. 6, pp. 1231-1233, 2003.
7. Erchak, A. A., Ripin, D. J., Fan, S. H., Rakich, P., Joannoupoulos, J. D., Ippen, E. P., Petrich, G. S. and Kolodziejski, L. A., "Enhanced coupling to vertical radiation using a two-dimensional photonic crystal in a semiconductor light-emitting diode," Appl. Phys. Lett., Vol. 78, No. 5, pp. 563-565, 2001.
8. Gao, W., "Precision nanometrology and its applications to precision nanosystems," Int. J. Prec. Eng. Manufac., Vol. 6, No. 4, pp. 14-20, 2005.
9. Song, C. K., Shin, Y. J. and Lee, H. S., "Performance assessment of an ultraprecision machine tool positioning system with a friction drive," Int. J. Prec. Eng. Manufac., Vol. 6, No. 3, pp. 8-12, 2005.
10. Kwon, K. H. and Cho, N. G, "Assessing the effect of stylus tip radius on surface roughness measurement by accumulation spectral analysis," Int. J. Prec. Eng. Manufac., Vol. 7, No. 1, pp. 9-12, 2006.
11. Chang, W. S., Choi, M. J., Kim, J. G, Cho, S. H. and Whang, K. H., "Thin film micromachining using femtosecond laser photo patterning of organic self-assembled monolayers," Int. J. Prec. Eng. Manufac., Vol. 7, No. 1, pp. 13-17, 2006.
12. Wierer, J. J., Krames, M. R., Epler, J. E., Gardner, N. F., Craford, M. G, Wendt, J. R., Simmons, J. A. and Sigalas, M. M., "InGaN/GaN quantum-well heterostructure light-emitting diodes employing photonic crystal structures," Appl. Phys. Lett., Vol. 84, No. 19, pp. 3885-3887, 2004.
13. Pasenow, B., Reichelt, M., Stroucken, T., Meier, T. and Koch, S. W., "Excitonic wave packet dynamics in semiconductor photonic-crystal structures," Phys. Rev. B, Vol. 71, pp. 195-321, 2005.
14. Veronis, G., Suh, W., Liu, Y., Han, M., Wang, Z., Dutton, R. W. and Fan, S., "Coupled optical and electronic simulations of electrically pumped photonic-crystal-based light-emitting diodes," J. Appl. Phys., Vol. 97, pp. 044503–044508, 2005.